NANO LETTERS

2007
Vol. 7, No. 3
685−689

Nanoparticle-Induced Fluorescence Lifetime Modification as Nanoscopic Ruler: Demonstration at the Single Molecule Level

J. Seelig,[†] K. Leslie,[‡] A. Renn,[†] S. Kühn,[†] V. Jacobsen,[†] M. van de Corput,[‡] C. Wyman,[§] and V. Sandoghdar*,[†]

Laboratory of Physical Chemistry, ETH Zürich, 8093 Zürich, Switzerland, Department of Cell Biology and Genetics, Erasmus Medical Centre, Rotterdam, The Netherlands, and Department of Radiation Oncology, Erasmus Medical Centre, Rotterdam, The Netherlands

Received November 25, 2006; Revised Manuscript Received January 30, 2007

ABSTRACT

We combine interferometric detection of single gold nanoparticles, single molecule microscopy, and fluorescence lifetime measurement to study the modification of the fluorescence decay rate of an emitter close to a nanoparticle. In our experiment, gold particles with a diameter of 15 nm were attached to single dye molecules via double-stranded DNA of different lengths. Nanoparticle-induced lifetime modification (NPILM) has promise in serving as a nanoscopic ruler for the distance range well beyond 10 nm, which is the upper limit of fluorescence resonant energy transfer (FRET). Furthermore, the simultaneous detection of single nanoparticles and fluorescent molecules presented in this work provides new opportunities for single molecule biophysical studies.

Optical methods provide versatile means for measuring distances, ranging from astronomical to angstrom dimensions. At the small scale, the wave nature of light and the principle of diffraction hamper resolving two point objects that are separated by $d < \lambda/2NA$, where λ is the wavelength of light and NA denotes the numerical aperture of the optics used. However, it has been shown that measurements in the near field can get around this diffraction limit because one has access to high spatial frequency components of the optical field.[1−3] In standard near-field microscopy, one scans a sharp probe to interrogate the near fields of a sample and is therefore limited to surface studies. An alternative for accessing near-field interactions is to integrate the "probe" into the sample so that a far-field reading of some property of the probe provides information about its near-field interaction with the object of interest. This is indeed the underlying principle of fluorescence resonant energy transfer (FRET),[4] where two fluorophores undergo dipole−dipole coupling so that the energy of the one (donor) is transferred to the other (acceptor). One can therefore learn about the separation of the donor and the acceptor by examining the amount of emission from the latter. Because the efficiency of this process scales as $1/(1 + (r/r_0)^6)$, it is significant over a very short distance range of $r_0 \sim 4-8$ nm for typical fluorophores.[5]

Another configuration of a built-in "nanoscopic ruler" exploits the near-field interaction of two metallic nanoparticles.[6,7] Although in general the interaction of the two particles is quite complex when considering all illumination polarizations, distance ranges, and particle sizes, the situation for very small particles can be understood as follows. Light induces oscillating dipole moments in each gold particle, and their instantaneous $(1/r)^3$ coupling results in a repulsive or attractive interaction, modifying the plasmon resonance of the system. The softer dependence of the interaction strength on the particle separation r results in a much longer interaction range compared to FRET. Very recently, a third possibility has been proposed in which the strength of fluorescence quenching and the accompanying change in the fluorescence lifetime act as measures for the separation between a fluorophore and metal clusters of diameter 1.5 nm.[8,9] In this case, sensitivity in displacements up to about 10−15 nm was demonstrated in ensemble measurements. Here we propose a generalized form of nanoparticle-induced lifetime modification (NPILM) and demonstrate its feasibility at the single molecule and single particle level. Our calcula-

* Corresponding author. E-mail: vahid.sandoghdar@ethz.ch.
[†] Laboratory of Physical Chemistry, ETH Zürich.
[‡] Department of Cell Biology and Genetics, Erasmus Medical Centre.
[§] Departments of Cell Biology and Genetics and of Radiation Oncology, Erasmus Medical Centre.

10.1021/nl0627590 CCC: $37.00
Published on Web 02/23/2007

tions show that nanoparticles of 5−40 nm in diameter provide sensitivity to small changes in the dye−particle distance even if they are separated by up to 40 nm. We also point out that NPILM can be applied also in nonmetallic systems where quenching is absent.

Modification of an emitter's excited-state decay rate due to its interaction with dielectric and metallic nanoparticles has been a subject of theoretical[10−13] and experimental[14−19] studies for more than two decades. As in the case of an emitter placed in front of a planar mirror,[20,21] the spontaneous emission rate can be shortened or lengthened, depending on the relative orientation of the dipole moment. Furthermore, particle size, geometry, and material strongly contribute to the fluorescence lifetime.[22] This phenomenon can be intuitively understood as the result of the interaction between the transition dipole moment of the emitter and its image dipole in the nanoparticle. In addition to this radiative effect, absorption in metallic nanoparticles opens loss channels and shortens the fluorescence lifetime at very close distances, leading to quenching.[9,16] Recently, we presented a controlled modification of the fluorescence intensity and the excited-state lifetime of a single molecule by scanning it against a single gold nanoparticle (diameter 100 nm) that was attached to the end of a glass fiber tip.[19] Furthermore, we have examined the modification of single molecule fluorescence close to various dielectric and metallic sharp tips.[23] In our current work, we study the fluorescence lifetime (τ) of a dye molecule that is spaced from a gold nanoparticle of diameter 15 nm by a double-stranded DNA (dsDNA) of various lengths, emphasizing the potential of NPILM for detecting distance variations in biophysical investigations.

Gold nanoparticles (GNP) are routinely used as labels in electron microscopy.[24] These particles can be fabricated in a large variety of sizes, are chemically stable, and are biocompatible. Gold nanoparticles also have very rich optical properties and have been studied very extensively.[25] If a GNP is much smaller than the wavelength of light, it acts as a Rayleigh scatterer and its far-field behavior can be modeled as that of a classical point dipole. It turns out that the dipolar polarizability of a GNP exhibits resonances, called plasmon-polaritons, which can be attributed to collective oscillations of the free electrons in the metal. Plasmon spectra are determined by several factors such as the size and shape of the GNP as well as the dielectric constant of their surrounding. For spherical GNPs of diameter less than 50 nm, as considered in this work, the plasmon resonance is centered at a wavelength of about 530−540 nm in water and is fairly insensitive to the particle size. Gold nanoparticles have also been studied for nearly three decades for their role in the enhancement of the Raman and fluorescence signals.[26] If the emitter is placed in the near-field of the GNP on its polarization axis where the local field is much larger than the incident field, the enhancement may be interpreted in terms of an optical antenna effect, which increases excitation and radiation of the emitter. In the reverse process, the antenna helps to radiate the excitation energy of the molecule more efficiently. The essence of these processes is quite similar to that of lifetime modification.

Recently, it has been shown that GNPs as small as 5 nm (or even smaller) can be detected by optical means.[27−31] The method of choice in our laboratory relies on the homodyne detection of the interference between the field scattered by the particle and a residual reflection as a reference beam. The details of this technique are discussed in refs 28, 31.

We have chosen to use dsDNA to space the GNP from a dye molecule. This choice is advantageous because the length of the spacer can be conveniently adjusted with 0.3 nm step size and because dsDNA is known to be rigid, having a persistence length of around 50 nm in low ionic strength buffer solutions.[32,33] To produce gold−DNA conjugates, we used thiolated DNA that would react with the surface of the gold particle (15 nm diameter, purchased from Aurion at concentration of 1.5×10^{12} particles per mL). For each experiment, DNA oligonucleotides (purchased from Eurogentec at a 0.05 μM scale) of defined length were used. We first annealed the 5′-thiolated DNA with its complement either with or without a 5′-Alexa label (10 mM Tris, pH 7.4, 1 mM EDTA). It was necessary to create GNP−DNA conjugates with one or a few Alexa-labeled DNA molecules. To achieve this, we varied the molar ratios of Alexa-labeled thiolated dsDNA and nonfluorescent thiolated DNA used in the GNP coupling reactions. Best results, in terms of eventual GNP solubility and frequency of single fluorescent DNA conjugated, were achieved with ratios of 100:1:10, unlabeled DNA:GNP:Alexa 532−DNA respectively. Reactions consisted of 50 μL of colloidal gold mixed with 25 μL of 500 nM thiolated unlabeled duplex and 2.5 μL of 500 nM thiolated Alexa 532 duplex. The final reaction volume was increased to 200 μL (with 22.5 μL of 10 mM TRIS, pH 7.4, 1 mM EDTA, and 100 μL of 20 mM Tris-HCL, pH 7.4, 100 mM NaCl, 5 mM EDTA, 0.05% Tween-20) and left at room temperature overnight. This produced GNP−DNA conjugates with 1−3 Alexa-conjugated DNA molecules and many unlabeled DNA molecules, increasing the overall solubility of the particles and preventing aggregation. Unbound Alexa-DNA left in the solution was removed by centrifugation and washing (16 g for 20 min followed by washing the pellet with 10 mM Tris-HCl, pH 7.4, 1 mM EDTA, repeated 3 times using 200 μL of TE buffer). The GNP−DNA conjugate was resuspended in a volume of 50 μL of buffer (10 mM Tris-HCl, pH 7.4, 1 mM EDTA).

For single molecule measurements, a buffer containing a dilute suspension of GNP−DNA constructs were added to the buffer in a liquid cell (volume = 60 μL) with an aminosilanized cover slide as the bottom floor. Immobilization of GNP−DNA complexes was achieved by adding 2−5 μL of 10 times diluted DNA−GNP solution prepared as described above, which resulted in a density of approximately 10−30 molecules per 100 μm^2 after a few minutes. Further adsorption was stopped by buffer exchange. All single molecule experiments were done in buffer at room temperature.

Figure 1 shows the schematics of our experimental setup based on a scanning stage confocal microscope. A solid-state pulsed laser (wavelength of 532 nm, pulse duration of about 30 ps, and a repetition rate of 75 MHz) was used to illuminate the sample through a high numerical aperture (*NA*

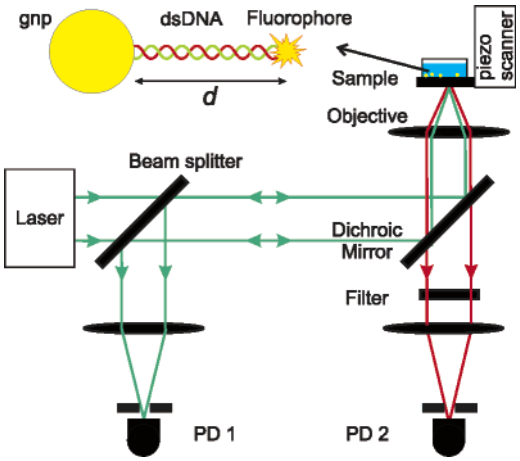

Figure 1. Schematics of the experimental setup. See text for details.

= 1.4) microscope objective. The average power used was about 1.6 μW, corresponding to an intensity of about 0.7 kW/cm^2 so that heating effects can be completely ignored.[27] A dichroic mirror in the detection channel directed light at the illumination wavelength to a photomultiplier (PD1) and sent the red-shifted fluorescence to an avalanche photodiode (PD2) after passing through a notch and a long-pass filter. This arrangement makes it possible to detect single gold nanoparticles[28,31] on PD1 and single fluorescent molecules on PD2 simultaneously.

The signal from the PD2 was fed to a time-correlated single photon counting module (Becker & Hickl SPC-402), allowing us to also record the fluorescence lifetime of single dye molecules. Figure 2a shows the signal contrast recorded on PD1 calculated according to $(I_{det} - I_{ref})/I_{ref}$, where I_{det} and I_{ref} denote the detected intensity and the intensity of the reflected light without any GNP, respectively. Figure 2b displays the simultaneously recorded fluorescence image on PD2. The arrows in Figure 2a mark the cases where fluorescence and scattering signals were co-localized within the laser focus spot. Although this co-localization is not a sufficient proof that only one dye molecule and one GNP are attached by a dsDNA, statistical data show that this is a very good assumption. To this end, we checked all our fluorescence data for single-step bleaching to ensure that we only considered signals from single molecules. As shown in Figure 2c, the signal contrast from 15 nm particles colocalized with single molecules followed a narrow distribution centered around −3% on PD1, indicating that the signals usually originate from single particles.[31] Spots with signal stronger than −6%, corresponding to two particles or more, were excluded from our analysis.

Once we identified GNP−molecule pairs, we centered the excitation laser beam on them and performed lifetime measurements. Figure 2d shows an example of the recorded lifetime curve. The single-exponential character of this typical plot and its good signal-to-noise ratio allow us to determine the fluorescence lifetime of this single molecule to be 0.63 ± 0.03 ns. We performed these measurements on six samples with different dsDNA lengths ranging from 44 to 112 base pairs, which correspond to the GNP−dye separation d = 17−40 nm after taking into account 1.8 nm for the lengths

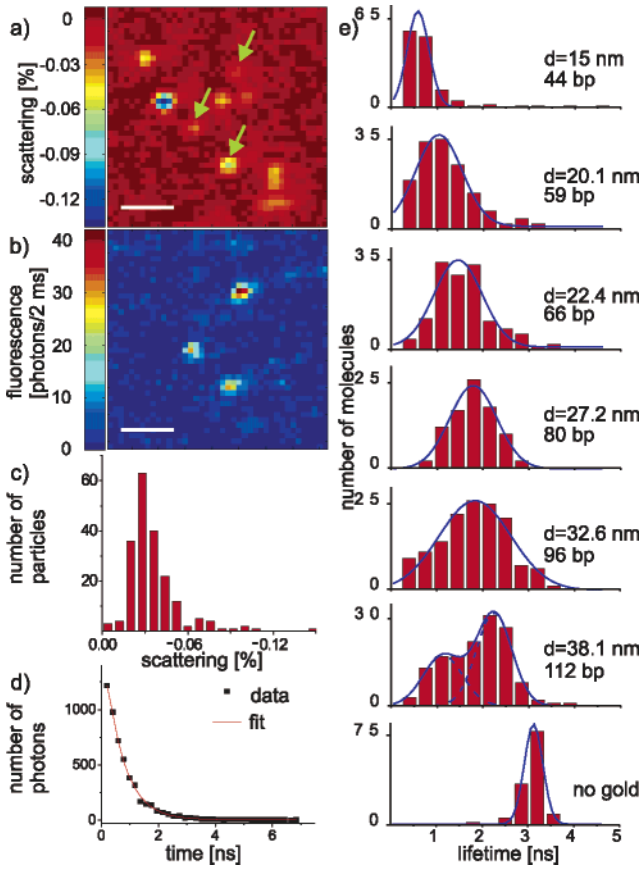

Figure 2. (a) Raster scan image of the scattering signal on PD1. (b) Fluorescence image recorded on PD2 simultaneously to (a). The scale bars correspond to 1 μm. The arrows in (a) show the cases of coincidence between a GNP and a dye molecule. (c) Histogram of the scattering signal, showing a narrow distribution about a contrast of −3%. (d) Example of a fluorescence decay trace from a single molecule. (e) A collection of the histograms of the recorded fluorescence lifetimes for six samples of different d and a reference sample without GNP.

of the GNP−thiol and DNA−dye linkers. In addition, we examined samples containing dsDNA−dye complex without any GNP as a reference. Figure 2e displays the distribution of the recorded lifetimes for more than 100 single molecules in each set. The distribution of the measured τ values follows a Gaussian function for nearly all cases, with a notable deviation for the case of d = 40 nm. The finite spread in τ can have various origins. First, variations in the orientation of the dye molecule as well as the size of the GNP influence τ. Also, the distance between the dye molecule and the closest point of GNP surface can vary, depending on whether the dsDNA is stretched along the tangent or along the normal to the GNP surface. We attribute the broadening of the distribution for the d = 34 nm data and the shoulder in the distribution of the d = 40 nm data to occasional shortening of the GNP−dye distance due to the interactions of the long DNA chains with the charged silanized surface.

The trend of the molecular excited-state lifetime as a function of its separation d from a GNP is evident in Figure 2e and is quantified in Figure 3a. In each case, the width of the Gaussian distribution in Figure 2e yields the assigned

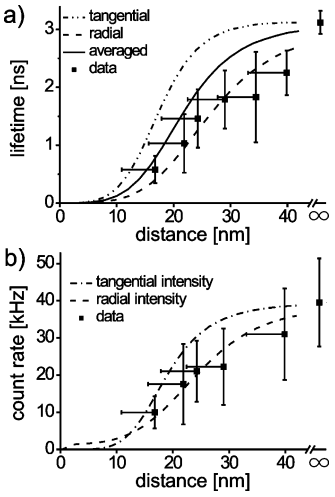

Figure 3. (a) Symbols show the average values of experimentally measured fluorescence lifetime of a large number of single molecules in samples for different d values. The last measurement was done in the absence of GNP and serves as a calibration. The dashed and dashed−dotted curves display the calculated fluorescence lifetime for the molecular dipole oriented radially or tangentially with respect to the GNP. The refractive index of the surrounding medium was taken to be $1.42 = (1.52 + 1.33)/2$ to account for the presence of the glass substrate in an approximative manner. The solid curve shows the weighted average of the two orientations. (b) Fluorescence signal corresponding to the measurements presented in part a).

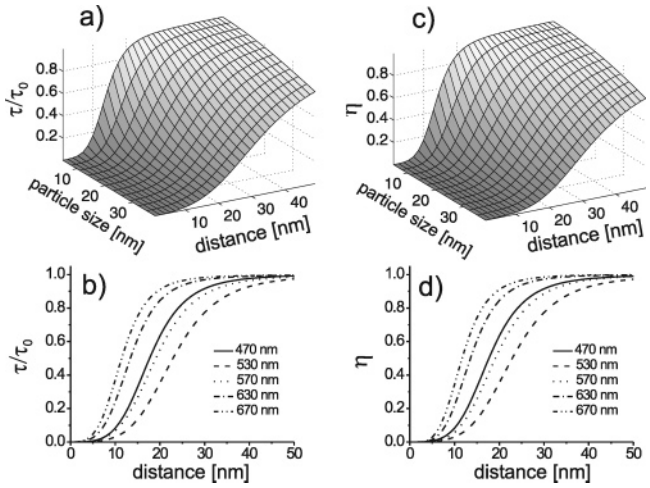

Figure 4. (a,c) Fluorescence lifetime τ normalized to the unperturbed lifetime τ_0 and quantum efficiency η of an emitter at different distances from the surface of a GNP of various diameters. (b,d) Normalized lifetime and quantum efficiency of an emitter placed at different separations from the surface of a GNP of diameter 15 nm and for various emission wavelengths.

vertical error bar. The asymmetric horizontal errors bars display the uncertainty in the distance between the dye and the GNP surface associated with the relative orientation of the dsDNA with respect to the GNP surface, as described above. We point out that the time jitter in the avalanche photodiode limited us to the smallest measurable τ of about 0.3 ns and thus prevented us from extending these measurements to much smaller d. In Figure 3a, we have also plotted the calculated lifetimes for both cases, where the molecular dipole is oriented radially or tangentially with respect to the GNP surface (see Supporting Information). We remark that our calculations do not take into account the influence of the interface between the glass substrate and water, but due to the weak refractive index contrast between glass (1.52) and water (1.33), it is reasonable to approximate the environment by a homogeneous medium of $n = 1.42$. The agreement between the experimental results and the theoretical predictions is very good within the experimental error, considering the lack of precise knowledge of the molecular dipole orientation. As seen in Figure 3, for a GNP of diameter 15 nm, the gradient of the curve and thus the sensitivity to changes in d is greatest in the range of $d \sim 15-25$ nm. For the system studied here, an error of 0.1 ns in the measurement of τ translates to an uncertainty of about 1 nm in determining the distance d, demonstrating the potential of NPILM as a nanoscopic ruler.

Figure 4a shows the calculated lifetime as a function of d for particles of diameter ranging from 5 to 40 nm. We note that one can tune the range and sensitivity of NPILM all the way from 5 nm, which is accessible to conventional FRET, to about 40 nm by choosing GNPs of different diameters. When choosing the experimental parameters for optimizing the NPILM signal, it is also important to take into account the effect of the GNP plasmon spectrum, which strongly affects the strength of the lifetime (τ) and quantum efficiency (η) modification.[19] Figure 4b plots τ for molecular emission at different wavelengths and as a function of separation d from a GNP with a diameter of 15 nm. It is evident that the interaction range of NPILM is longer when the emission wavelength coincides with the plasmon resonance (dashed lines).

As pointed out earlier, the change in the fluorescence lifetime close to a metallic nanoparticle can be due to the modification of the spontaneous emission or due to quenching. The latter results in a lower quantum efficiency and thus a lower emission rate. Figure 4c shows η as a function of the particle size and of d, while Figure 4d displays the dependence of η on the emission wavelength and on d, again for a 15 nm large GNP. The strong resemblance of parts a,b and c,d of Figure 4 let us conclude that, for the parameters (GNP size and d) of our current experiment, the dominant process of lifetime modification has been quenching. This is in accord with the observation that, as shown in Figure 3b, the fluorescence intensity diminishes as d becomes smaller. The solid curves in this figure display the expected distance dependence of the fluorescence signal when taking into account both excitation enhancement and the change in the quantum efficiency (see ref 19 for more detailed discussion on this issue) and are in good agreement with the recorded data.

We now remark on several features of the system presented here. First, as in FRET, rotation of the molecule can lead to a change in the fluorescence lifetime, introducing a systematic error in the assessment of a translational motion between the molecule and the GNP. An advantage of NPILM is however that this effect is less disruptive than in FRET because a rotation in the plane tangential to the GNP does not affect τ. The greatest promise of NPILM lies in its ability to reveal real-time motion in nanoscopic biological entities.

It has been shown that one can comfortably determine the fluorescence lifetime at an accuracy of 10% with about 200 detected photons or 3% with about 5000 photons.[34] In this context, we note that, according to our observations, the total number of emitted photons per molecule has been the same for all samples, indicating that photobleaching activities have not been affected by the presence of the GNP. Next, we point out that, as indicated by Figure 3b, the change in d is also revealed in the overall fluorescence signal if quenching is the dominant interaction mechanism.[8] However, measuring fluorescence lifetime has the advantage that it is insensitive to fluorescence blinking and does not depend on the excitation intensity, which could be enhanced or suppressed depending on the polarization of light and the geometry of the particle. Finally, we emphasize that NPILM is not limited to quenching and could also be realized using dielectric nanoparticles[10,11] or at larger distances from larger metallic nanoparticles,[19] where the change in τ is dominated by the modification of the spontaneous emission rate.

In conclusion, we have investigated the excited-state decay rate of a fluorophore attached to a gold nanoparticle at the single molecule and single particle level. The distance dependence of this phenomenon can be engineered by choosing the size of the nanoparticle and serves as a nanoscopic ruler for measuring distances beyond what is accessible to FRET. The method presented here can also trigger other new but related arrangements for the study of motional dynamics at the nanometer scale. For example, gold nanoparticles can be used in combination with standard FRET whereby the GNP is used to modify the fluorescence lifetimes of the donor and acceptor molecules and therefore the rate of energy transfer between the two.[38] For this configuration, the GNP can be as large as about 100 nm and can be considered as a special substrate for FRET studies As we have shown in a recent publication, in this system, quenching can be compensated by the strong enhancement of the excitation electric field[19,35] if the distance d is chosen properly. Furthermore, by designing more efficient optical nanoantennas and tailoring their plasmon resonances, one could considerably enhance the sensitivity of this method. Another promise of the experimental approach discussed in this work is colocalization of two nano-objects by simultaneous detection of the fluorescence and the scattering of individual nanoparticles. We emphasize that the latter method is not restricted to metallic objects and can be generalized to biological nano-objects such as microtubules and viruses.[31,36,37]

Acknowledgment. This work was performed within the frame of an Integrated Project of the European Union "Molecular Imaging". We also acknowledge financial support by the ETH Zurich and the Swiss National Foundation (SNF). We thank Lavinia Rogobete for her contributions to the preliminary calculations.

Supporting Information Available: Description of the theoretical treatment of the modification of the radiative and nonradiative decay rates as well as the fluorescence intensity of an emitter close to a spherical nanoparticle. This material is available free of charge via the Internet at http://pubs.acs.org.

References

(1) Pohl, D. W.; Denk, W.; Lanz, M. *Appl. Phys. Lett.* **1984**, *44*, 651.
(2) Lewis, A.; Isaacson, M.; Harootunian, A.; Murray, A. *Ultramicroscopy* **1984**, *13*, 27.
(3) Sandoghdar, V. *Proceedings of the International School of Physics*; IOS Press: Amsterdam, 2001; pp 65−119.
(4) Förster, T. *Ann. Phys.* **1948**, *6*, 55.
(5) Lakowicz, J. R. *Principles of Fluorescence Spectroscopy* 2nd ed.; Kluwer Academic, Plenum Publishers: New York, 1999.
(6) Quinten, M. *Appl. Phys. B* **1998**, *67*, 101.
(7) Reinhard, B. M.; Siu, M.; Agarwal, H.; Alivisatos, A. P.; Liphardt, J. *Nano Lett.* **2005**, *5*, 2246.
(8) Yun, C. S.; Javier, A.; Jennings, T.; Fisher, M.; Hira, S.; Peterson, S.; Hopkins, B.; Reich, N. O.; Strouse, G. F. *J. Am. Chem. Soc.* **2005**, *127*, 3115.
(9) Jennings, T. L.; Singh, M. P.; Strouse, G. F. *J. Am. Chem. Soc.* **2006**, *128*, 5462.
(10) Chew, H. *J. Chem. Phys.* **1987**, *87*, 1355.
(11) Klimov, V. V.; Ducloy, M.; Letokhov, V. S. *J. Mod. Opt.* **1996**, *43*, 2251.
(12) Ruppin, R. *J. Chem. Phys.* **1982**, *76*, 1681.
(13) Rogobete, L.; Schniepp, H.; Sandoghdar, V.; Henkel, C. *Opt. Lett.* **2003**, *28*, 1736.
(14) Geddes, C. D.; Lakowicz, J. R. *J. Fluoresc.* **2002**, *12*, 121.
(15) Schniepp, H.; Sandoghdar, V. *Phys. Rev. Lett.* **2002**, *89*, 257403.
(16) Dulkeith, E.; Morteani, A. C.; Niedereichholz, T.; Klar, T. A.; Feldmann, J.; Levi, S. A.; van Veggel, F. C. J. M.; Reinhoudt, D. N.; Möller, M.; Gittins, D. I. *Phys. Rev. Lett.* **2002**, *89*, 203002.
(17) Dulkeith, E.; Ringler, M.; Klar, T. A.; Feldmann, J.; Javier, A. M.; Parak, W. J. *Nano Lett.* **2005**, *5*, 585.
(18) Gueroui, Z.; Libchaber, A. *Phys. Rev. Lett.* **2004**, *93*, 166108.
(19) Kühn, S.; Håkanson, U.; Rogobete, L.; Sandoghdar, V. *Phys. Rev. Lett.* **2006**, *97*, 017402.
(20) Drexhage, K. H. *Prog. Opt.* **1974**, *12*, 165.
(21) Chance, R. R.; Prock, A.; Silbey, R. *Adv. Chem. Phys.* **1978**, *37*, 1.
(22) Klimov, V. V.; Ducloy, M.; Letokhov, V. S. *Quantum Electron.* **2001**, *31*, 569.
(23) Kühn, S.; Sandoghdar, V. *Appl. Phys. B* **2006**, *84*, 211.
(24) Horisberger, M.; Rosset, J. *J. Histochem. Cytochem.* **1977**, *25*, 295.
(25) Kreibig, U.; Vollmer, M. *Optical Properties of Metal Clusters*; Springer: Berlin, 1995.
(26) Metiu, H. *Prog. Surf. Sci.* **1984**, *17*, 153.
(27) Boyer, D.; Tamarat, P.; Maali, A.; Lounis, B.; Orrit, M. *Science* **2002**, *297*, 1160.
(28) Lindfors, K.; Kalkbrenner, T.; Stoller, P.; Sandoghdar, V. *Phys. Rev. Lett.* **2004**, *93*, 037401.
(29) Arbouet, A.; Christofilos, D.; Fatti, N. D.; Vallée, F.; Huntzinger, J. R.; Arnaud, L.; Billaud, P.; Broyer, M. *Phys. Rev. Lett.* **2004**, *93*, 127401.
(30) Berciaud, S.; Cognet, L.; Blab, G. A.; Lounis, B. *Phys. Rev. Lett.* **2004**, *93*, 257402.
(31) Jacobsen, V.; Stoller, P.; Brunner, C.; Vogel, V.; Sandoghdar, V. *Opt. Express* **2006**, *14*, 405.
(32) Record, J. M. T.; Mazur, S. H.; Melancon, P.; Roe, J.-H.; Shaner, S. L.; Unger, L. *Annu. Rev. Biochem.* **1981**, *50*, 997.
(33) Lu, Y.; Weers, B.; Stellwagen, N. C. *Biopolymers* **2002**, *61*, 261.
(34) Kollner, M.; Wolfrum, J. *Chem. Phys. Lett.* **1992**, *200*, 199.
(35) Anger, P.; Bharadwaj, P.; Novotny, L. *Phys. Rev. Lett.* **2006**, *96*, 113002.
(36) Ignatovich, F. V.; Novotny, L. *Phys. Rev. Lett.* **2006**, *96*, 013901.
(37) Jacobsen, V.; Klotzsch, E.; Sandoghdar, V. In *Nano Biophotonics (Handai Nanophotonics Series Vol. 3)*; Masuhara, H., Kawata, S., Tokunaga, F., Eds.; Elsevier: New York, 2007.
(38) It was brought to our attention in the reviewing process that a similar idea has been discussed in a new publication by Zhang, J.; Fu, Y.; Lakowicz, J. R. *J. Phys. Chem. C* **2007**, *111*, 50.

NL0627590